

High-Nuclearity Silver Thiolate Clusters Constructed with Phosphonates

Yun-Peng Xie,* Jun-Ling Jin, Xing Lu,* and Thomas C. W. Mak

Abstract: The *n*-butylphosphonate ligand has been employed to construct three new silver(I) thiolate compounds. Single-crystal X-ray analysis revealed that complexes **1** and **2** are Ag₄₈ and Ag₅₁ coordination chain polymers, while **3** contains a discrete Ag₄₈ cluster, in which three different kinds of silver(I) thiolate cluster shells enclose three different phosphonate-functionalized silver(I) cluster cores, respectively. The structures of clusters in **1–3** feature three three-shell arrangements, S@Ag₁₂@(nBuPO₃)₉@Ag₃₆S₂₃, S@Ag₁₁@(nBuPO₃)₇(MoO₄)₂@Ag₄₀S₂₇ and MoO₄@Ag₁₂@(nBuPO₃)₈S₆@Ag₃₆S₂₄, respectively.

The chemistry of metal clusters has attracted much interest in view of their structural diversity and potential use for applications.^[1] Among them, high-nuclearity silver(I) clusters constitute an intriguing subclass that has been studied extensively.^[2] Recently, many high-nuclearity silver(I) thiolate clusters have been separately prepared and structurally characterized.^[3] Some of the Ag nanoclusters have been found to exhibit excellent luminescence properties^[3c,d] and ultrastability.^[3e,f] On the other hand, metal phosphonates vary in structural form from discrete molecules to multidimensional coordination polymers,^[4,5] which have potential applications in ion exchange, catalysis, and chemical sensing.^[6] Recently we employed *t*BuPO₃H₂ as a precursor to react with AgC≡CR to construct a series of high-nuclearity silver(I)–ethynide cluster compounds,^[7] in which the *t*BuPO₃^{2–} unit constitutes a structural component for building up the cluster shell,^[7a–c] functions as a tripodal strut to support vertex-sharing or fusion of two small silver(I) clusters to form an enlarged composite cluster.^[7d]

In contrast to silver(I)–ethynide clusters, there are as yet no reported examples of silver(I) thiolate clusters constructed with phosphonates. Thus, new synthetic routes, especially those employing phosphonates as precursors, are worth

exploring because they may lead to the assembly of unique high-nuclearity phosphonate-functionalized silver(I) thiolate clusters.

In this work, two unprecedented 1D assemblies, {[S@Ag₁₂@(nBuPO₃)₉@Ag₃₆(*t*BuS)₂₃(CH₃O)₂(NO₃)₃]·2CH₃OH}_n (**1**) and {[S@Ag₁₁@(nBuPO₃)₇(MoO₄)₂@Ag₄₀(*t*BuS)₂₇(CH₃O)₂(NO₃)₂(H₂O)₂]·8CH₃OH·1.5H₂O}_n (**2**), and an anionic cluster [CH₃OH₂]₆[MoO₄@Ag₁₂@(nBuPO₃)₈S₆@Ag₃₆(*t*BuS)₂₄] (**3**) based on silver(I) thiolate cages as their surface components and phosphonate-functionalized silver(I) clusters as their cores, have been isolated and structurally characterized by single-crystal X-ray crystallography.

The reaction of *t*BuSAg, *n*BuPO₃H₂, AgBF₄/AgNO₃, and a small amount of TMEDA (*N,N,N',N'*-tetramethyl-ethylenediamine) in methanol/dichloromethane afforded yellow crystals of {[S@Ag₁₂@(nBuPO₃)₉@Ag₃₆(*t*BuS)₂₃(CH₃O)₂(NO₃)₃]·2CH₃OH}_n (**1**). Single-crystal X-ray analysis^[8] revealed that complex **1** is a 1D assembly consisting of Ag₄₈ clusters bridged by NO₃[–] anions (Supporting Information, Figure S1). The fundamental building unit of **1** can be regarded as a nanosized core-shell configuration, in which a silver thiolate cluster shell [Ag₃₆(*t*BuS)₂₃]¹³⁺ wraps around a phosphonate-functionalized silver(I) cluster core [Ag₁₂(*n*BuPO₃)₉]^{6–}, which in turn encapsulates a sulfide ion template (Figures 1 and 2). The central S^{2–} ion generated from S–C bond cleavage of the *t*BuS– ligand uses a μ₆-ligation mode to coordinate to six silver atoms of its surrounding Ag₁₂ unit, with Ag–S lengths varying from 2.465 to 2.531 Å

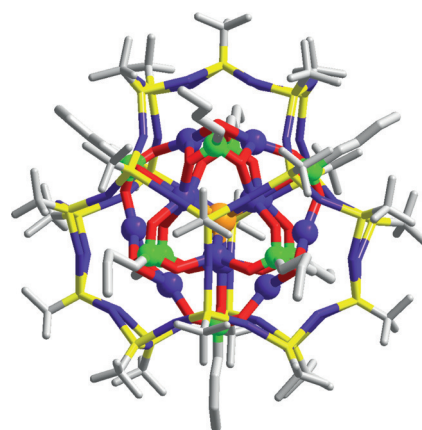


Figure 1. Perspective view showing the core-shell configuration of the nanocluster in complex **1**. All hydrogen atoms and bonds between [Ag₃₆(*t*BuS)₂₃]¹³⁺ and [S@Ag₁₂(*n*BuPO₃)₉]^{6–}, CH₃O[–], NO₃[–], and CH₃OH are omitted for clarity. The enclosed sulfide ion is represented by a large light orange sphere. Color code: Ag, violet; S (thiolate) yellow; S^{2–}, light orange; P, green; O, red; C, gray.

[*] Dr. Y.-P. Xie, Prof. X. Lu
State Key Laboratory of Materials Processing and
Die and Mould Technology
School of Materials Science and Engineering
Huazhong University of Science and Technology (HUST)
Wuhan 430074 (China)
E-mail: xieyp@hust.edu.cn
lux@hust.edu.cn

Prof. T. C. W. Mak
Department of Chemistry and Center of Novel Functional Molecules
The Chinese University of Hong Kong
Shatin, New Territories, Hong Kong SAR (P.R. China)

Supporting information and ORCID(s) from the author(s) for this article are available on the WWW under <http://dx.doi.org/10.1002/anie.201507512>.

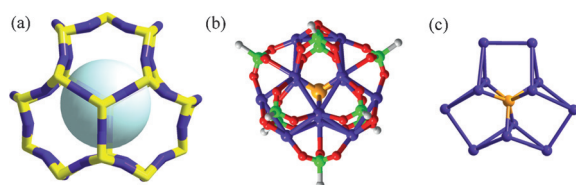


Figure 2. a) The $[\text{Ag}_{36}(\text{tBuS})_{23}]^{3+}$ shell structure of **1** with all peripheral *tert*-Bu groups omitted for clarity, and the large white sphere shows the inner space occupied by the $\text{S}@\text{Ag}_{12}$ cluster core. b) Perspective view of the anionic $[\text{S}@\text{Ag}_{12}(\text{nBuPO}_3)_9]^{8-}$ cluster. Hydrogen atoms are omitted, and only carbon atoms bound to phosphorus atoms are shown. c) Perspective view of the $\text{S}@\text{Ag}_{12}$ cluster core. Color code: Ag, violet; S (thiolate), yellow; S^{2-} , light orange; P, green; O, red; C, gray.

(Figure 2c). The structure of the Ag_{12} unit can be regarded as a compressed triangular orthobicupola that is consolidated by nine *n*-butylphosphonates (Figure 2b). On the other hand, the Ag_{12} unit is further attached to an outer $[\text{Ag}_{36}(\text{tBuS})_{23}]^{13+}$ shell through the nine *n*-butylphosphonates, which adopt $\mu_7\text{-}\eta^2, \eta^2, \eta^3$, $\mu_9\text{-}\eta^3, \eta^3, \eta^3$, $\mu_{12}\text{-}\eta^4, \eta^4, \eta^4$ ligation modes to coordinate to silver atoms from the Ag_{12} core and $\text{Ag}_{36}\text{S}_{23}$ shell, with the Ag-O_p (O_p = oxygen atom of the *n*-butylphosphonate ligand) bond distances in the range of 2.120–2.783 Å (Figure S2).

In the outer cationic $[\text{Ag}_{36}(\text{tBuS})_{23}]^{13+}$ cluster, twenty-three *tBuS*[−] ligands, twenty adopting the $\mu_3\text{-}\eta^1, \eta^1, \eta^1$ ligation mode and the other three using the $\mu_4\text{-}\eta^1, \eta^1, \eta^1, \eta^1$ mode, build a $\text{Ag}_{36}\text{S}_{23}$ cluster shell containing nine Ag–S dodecagons and six hexagons, with Ag–S bond lengths varying from 2.260 to 2.543 Å (Figure 2a). Two CH_3O^- and one NO_3^- anion also function as terminal ligands to coordinate to silver atoms.

Adjacent $[\text{S}@\text{Ag}_{12}(\text{nBuPO}_3)_9]^{8-}$ and $[\text{Ag}_{36}(\text{tBuS})_{23}(\text{CH}_3\text{O})_2(\text{NO}_3)_2]^{2+}$ clusters are further extended into zigzag chains bridged by nitrate anions, with Ag– O_N bond lengths varying from 2.538 to 2.551 Å (Figure S1). The crystal structure also contains two solvated methanol molecules in the unit cell.

The synthesis procedure used to obtain $[\{\text{S}@\text{Ag}_{11}(\text{nBuPO}_3)_7(\text{MoO}_4)_2\}@\text{Ag}_{40}(\text{tBuS})_{27}(\text{CH}_3\text{O})_2(\text{NO}_3)_2(\text{H}_2\text{O})_2] \cdot 8\text{CH}_3\text{OH} \cdot 1.5\text{H}_2\text{O}$ (**2**) is similar to that used for **1**, except that $\text{MoO}_2(\text{acac})_2$ is added to the reaction mixture. Complex **2** exhibits a linear assembly of Ag_{51} cluster units bridged by NO_3^- anions (Figure S3). The fundamental building unit of **2** comprises a cationic $[\text{Ag}_{40}(\text{tBuS})_{27}]^{13+}$ cluster shell consolidated by two nitrate anions, two CH_3O^- ligands, and two water molecules, which encapsulates an inner $[\text{S}@\text{Ag}_{11}(\text{nBuPO}_3)_7(\text{MoO}_4)_2]^{9-}$ cluster (Figures 3 and 4). The central sulfido S atom coordinates to six silver atoms from its Ag_{11} envelope, with Ag–S lengths varying from 2.498 to 2.565 Å. The Ag_{11} unit can be described as consisting of a butterfly-shaped Ag_4 unit and a Ag_7 aggregate comprising two butterfly-shaped Ag_4 units coalesced by sharing one vertex (Figure 4c). The Ag_{11} unit is stabilized and further attached to the outermost $[\text{Ag}_{40}(\text{tBuS})_{27}]^{13+}$ shell through seven *n*-butylphosphonates and two molybdates (Figure 4b). Of the *n*-butylphosphonates, one adopts the $\mu_7\text{-}\eta^2, \eta^2, \eta^3$ bridging mode, and the remaining six use $\mu_9\text{-}\eta^3, \eta^3, \eta^3$ ligation modes to coordinate to Ag atoms belonging to the Ag_{11} core and Ag_{40} shell, with Ag– O_p bonds in the range of 2.126–2.600 Å. However, each of the two $[\text{MoO}_4]^{2-}$ anions derived from

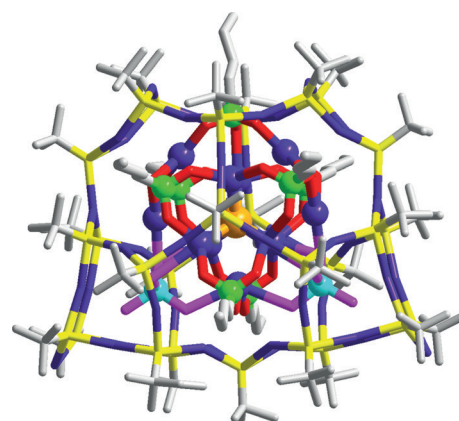


Figure 3. Perspective view of the core-shell configuration of the nano-cluster in complex **2**. All hydrogen atoms and bonds between $[\text{Ag}_{40}(\text{tBuS})_{27}]^{13+}$ and $[\text{S}@\text{Ag}_{11}(\text{nBuPO}_3)_7(\text{MoO}_4)_2]^{9-}$, CH_3O^- , NO_3^- , CH_3OH , and H_2O are omitted for clarity. The enclosed sulfide ion is represented by a large light orange sphere. Color code: Ag, violet; Mo, sky blue; S (thiolate), yellow; S^{2-} , light orange; P, green; O, red; C, gray.

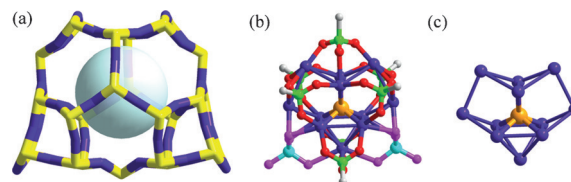


Figure 4. a) The $[\text{Ag}_{40}(\text{tBuS})_{27}]^{13+}$ shell structure of **2** with all peripheral *tert*-Bu groups omitted for clarity, and the large turquoise sphere shows the inner space occupied by the $\text{S}@\text{Ag}_{11}$ core unit. b) Perspective view of the anionic $[\text{S}@\text{Ag}_{11}(\text{nBuPO}_3)_7(\text{MoO}_4)_2]^{9-}$ cluster. Hydrogen and carbon atoms are omitted; only carbon atoms bound to phosphorus atoms are shown. c) Perspective view of the innermost $\text{S}@\text{Ag}_{11}$ cluster core. Color code: Ag, violet; Mo, sky blue; S (thiolate), yellow; S^{2-} , light orange; P, green; C, gray; O (*n*-butylphosphonate), red; O (molybdate), purple.

$\text{Mo}(\text{acac})_2$ adopts the $\mu_{13}\text{-}\eta^3, \eta^3, \eta^3, \eta^4$ bridging mode to coordinate to thirteen silver atoms, with the Ag-O_M (O_M = molybdate oxygen atom) bond in the range of 2.270–2.855 Å (Figure S4).

As compared to **1**, various Ag–S polygons, including two hexagons, six octagons, two decagons, and seven dodecagons are present in the outer cationic $[\text{Ag}_{40}(\text{tBuS})_{27}]^{13+}$ cluster in **2** (Figure 4a). Of the 27 *tBuS*[−] ligands that bind the Ag_{40} cluster together, 26 adopt $\mu_3\text{-}\eta^1, \eta^1, \eta^1$ ligation modes to link three silver atoms, and the remaining one uses the $\mu_4\text{-}\eta^1, \eta^1, \eta^1, \eta^1$ mode to coordinate to four silver atoms, with Ag–S bond lengths varying from 2.374 to 2.504 Å. Two CH_3O^- anions and two water molecules each coordinate to only one silver atom.

Adjacent $[\text{S}@\text{Ag}_{11}(\text{nBuPO}_3)_7(\text{MoO}_4)_2]^{9-}$ and $[\text{Ag}_{40}(\text{tBuS})_{27}(\text{CH}_3\text{O})_2(\text{H}_2\text{O})_2]^{2+}$ clusters are further extended into zigzag chains bridged by nitrate anions, with Ag– O_N lengths varying from 2.320 to 2.715 Å. The crystal structure also contains solvated methanol and water molecules that partake in hydrogen bonding.

The generation of complexes **1** and **2** is evidence that AgNO_3 plays a critical role. To restrict the formation of chains and control the assembly progress, $\text{AgBF}_4/\text{AgNO}_3$ reactants were replaced by AgBF_4 in the synthetic procedure, and a cluster compound, $[\text{CH}_3\text{OH}_2]_6 \{ \text{MoO}_4 @ \text{Ag}_{12} @ (\text{nBuPO}_3)_8 \text{S}_6 @ \text{Ag}_{36} (\text{tBuS})_{24} \}$ (**3**) was successfully isolated. Single-crystal X-ray analysis showed that complex **3** is an anionic forty-eight nuclear silver cluster (Figure 5). In complex **3**, a molybdate

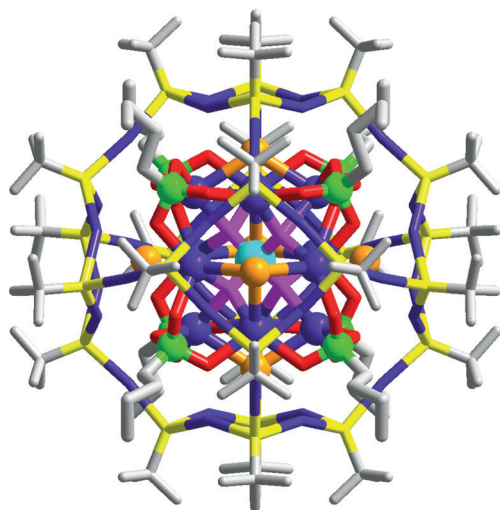


Figure 5. Perspective view of the core-shell configuration of the nano-cluster in complex **3**. All hydrogen atoms and bonds between $[\text{Ag}_{36}(\text{tBuS})_{24}]^{12+}$ and $[\text{MoO}_4 @ \text{Ag}_{12} (\text{nBuPO}_3)_8 \text{S}_6]^{18-}$ are omitted for clarity. Color code: Ag, violet; Mo, sky blue; S (thiolate), yellow; S^{2-} , light orange; P, green; O, red; C, gray.

$[\text{MoO}_4]^{2-}$ template anion is encapsulated within an anionic $[\text{Ag}_{12}(\text{nBuPO}_3)_8 \text{S}_6]^{16-}$ cluster composed of twelve silver(I) ions, eight $[\text{nBuPO}_3]^{2-}$ units, and six S^{2-} anions, which is in turn covered by a cationic $[\text{Ag}_{36}(\text{tBuS})_{24}]^{12+}$ cluster surface. The templating $[\text{MoO}_4]^{2-}$ anion exhibits twofold orientational disorder with each set of O atoms having half occupancy, and adopts a tetrahedral topology. Each oxygen atom in $[\text{MoO}_4]^{2-}$ anion is bound to three silver atoms in $\mu_3\text{-}\eta^1, \eta^1, \eta^1$ ligation mode to build the $\{ \text{MoO}_4 @ \text{Ag}_{12} \}$ structure, with Ag–O bond lengths of 2.355 and 2.397 Å (Figure 6c). The Ag_{12} unit can be

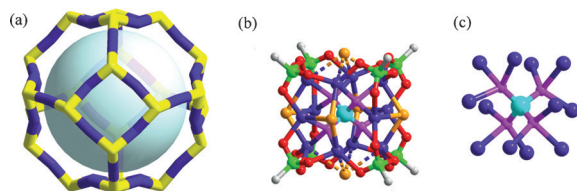


Figure 6. a) The $[\text{Ag}_{36}(\text{tBuS})_{24}]^{12+}$ shell structure of **3** with all peripheral *tert*-Bu groups omitted for clarity, and the large turquoise sphere shows the inner space occupied by the $\text{MoO}_4 @ \text{Ag}_{12}$ cluster core. b) Perspective view of the anionic $[\text{MoO}_4 @ \text{Ag}_{12} (\text{nBuPO}_3)_8 \text{S}_6]^{18-}$ cluster. Hydrogen and carbon atoms are omitted, only carbon atoms bound to phosphorus atoms are shown. c) Perspective view of the $\text{MoO}_4 @ \text{Ag}_{12}$ cluster core. Color code: Ag, violet; Mo, sky blue; S (thiolate), yellow; S^{2-} , light orange; P, green; C, gray; O (n-butylphosphonate), red; O (molybdate), purple.

regarded as a distorted cuboctahedron composed of eight triangles and six squares. In **3**, the six squares faces of the cuboctahedron are capped by six S^{2-} ligands, and the eight triangular faces are stabilized by eight $[\text{nBuPO}_3]^{2-}$ ions (Figure 6b). The structure of $[\text{Ag}_{12}(\text{nBuPO}_3)_8]$ is related to the previously studied metal clusters.^[5b,9] On the other hand, the $[\text{MoO}_4 @ \text{Ag}_{12}]$ cluster is further attached to the outer shell by the six S^{2-} and the eight $[\text{nBuPO}_3]^{2-}$ ions (Figure 6b). As a result, four S^{2-} ions adopt the μ_5 -bridging mode to link Ag atoms of from the Ag_{12} core to the Ag_{36} shell, with Ag–S bonds in the range of 2.829–2.931 Å, while the remaining two S^{2-} ions are weakly bonded to four silver atoms from the Ag_{36} shell with the Ag–S bond length being 3.070 Å. Three oxygen atoms in each $[\text{nBuPO}_3]^{2-}$ anion coordinate to seven silver(I) ions, with Ag–O_p bond lengths varying from 2.233 to 2.830 Å.

In the outer cationic $[\text{Ag}_{36}(\text{tBuS})_{24}]^{12+}$ cluster, twenty-four *t*BuS[−] ligands, each adopting $\mu_3\text{-}\eta^1, \eta^1, \eta^1$ ligation mode, build an $\text{Ag}_{36}\text{S}_{24}$ cluster shell containing eight Ag–S dodecagons and six octagons, with Ag–S bond lengths varying from 2.358 to 2.425 Å (Figure 6a). From **3** we can conclude that the template anion MoO_4^{2-} has a significant influence on the symmetry and the structure of the Ag cluster. Overall charge balance against the giant anionic cluster is provided by six protonated methanol molecules in molecular packing, which was observed previously in other structures.^[10]

The syntheses and structural characterization of **1–3** showed that large phosphonate-functionalized silver(I) thiolate clusters can be built up by an assembly process in solution. For **1** and **2**, under suitable reaction conditions, each of two silver(I) clusters that encapsulates a sulfide ion can, in turn, act as a cationic template to induce the formation of a large Ag–S cluster shell. The synthesis of **2** involving addition of $\text{MoO}_2(\text{acac})_2$ could present a procedure for incorporating $[\text{MoO}_4]^{2-}$ into Ag^{I} cluster. In **1**, the Ag_{36} cluster cavity accommodates the $[\text{S} @ \text{Ag}_{12}(\text{nBuPO}_3)_9]^{8-}$ cluster, whereas in **2** the much larger Ag_{40} cluster cavity encloses a $[\text{S} @ \text{Ag}_{11}(\text{nBuPO}_3)_7(\text{MoO}_4)_2]^{9-}$ cluster. As compared to **1**, two $[\text{nBuPO}_3]^{2-}$ units are replaced by two $[\text{MoO}_4]^{2-}$ units in **2**, and more oxygen atoms are available for coordination to the surface silver(I) atoms through Ag–O bonding interactions. The present assembly reaction is also influenced by the choice of the inorganic anions: when silver tetrafluoroborate and silver nitrate were replaced by silver tetrafluoroborate in the synthetic procedure, cluster complex **3** was deposited instead of coordination polymers of **1** and **2**.

The successive buildup of clusters **1–3** is associated with template ions. The topology structures of clusters in **1** and **2** feature three-shell arrangements, $\text{S} @ \text{Ag}_{12} @ (\text{nBuPO}_3)_9 @ \text{Ag}_{36}\text{S}_{23}$ and $\text{S} @ \text{Ag}_{11} @ (\text{nBuPO}_3)_7(\text{MoO}_4)_2 @ \text{Ag}_{40}\text{S}_{27}$, respectively, in which the S^{2-} anion is encapsulated as a template. Through variation of the reaction conditions, we successively obtained an fascinating topological structure of **3**, $\text{MoO}_4 @ \text{Ag}_{12} @ (\text{nBuPO}_3)_8 \text{S}_6 @ \text{Ag}_{36}\text{S}_{24}$, in which the MoO_4^{2-} anion is enclosed as a template.

In summary, we have synthesized and structurally characterized two unprecedented 1D assemblies and an anionic cluster based on silver(I) thiolate cages as their surface components and phosphonate-functionalized silver(I) clusters as cores. For the first time, the *n*-butylphosphonate

component is used to build up high-nuclear silver(I) thiolate clusters. Their beautiful motif structures feature a three-shell arrangement with an innermost template anion (S^{2-} for **1** and **2**, MoO_4^{2-} for **3**): in succession, Ag cluster, *n*-butylphosphonate ligands (also including molybdates for **2**), and a Ag–S cluster. The present study opens the way to synthetic studies of silver(I) thiolate clusters employing potential precursors exemplified by phosphonic and arsonic acids.

Experimental Section

*t*BuSAg was prepared from the reaction of equivalent amounts of $AgNO_3$ and *t*BuSH in Et_3N . Other reagents and solvents were obtained from commercial sources and used without further purification. Elemental analyses for C, H, and N were performed with a PerkinElmer 2400 CHN elemental analyzer.

1: *t*BuSAg (0.035 g, 0.18 mmol), $AgBF_4$ (0.002 g, 0.01 mmol) and $AgNO_3$ (0.002 g, 0.012 mmol) were dissolved in 6 mL methanol and dichloromethane under ultrasonication; then TMEDA (0.001 g, 0.008 mmol) was added under stirring to form a clear yellow solution, to which $nBuPO_3H_2$ (0.005 g, 0.036 mmol) was added under stirring. The resulting mixture was allowed to stand at room temperature for 24 h, and a yellow solution was collected by filtration. Slow evaporation of this solution afforded the product as yellow crystals. Yield: ca. 28 % (based on $nBuPO_3H_2$). Elemental analysis (%) calcd for $C_{132}H_{302}N_3P_9S_{24}Ag_{48}$: C 19.44, H 3.73, N 0.52; found: C 19.67, H 3.94, N 0.41.

2: *t*BuSAg (0.035 g, 0.18 mmol), $AgBF_4$ (0.002 g, 0.01 mmol) and $AgNO_3$ (0.002 g, 0.012 mmol) were dissolved in 6 mL methanol and dichloromethane under ultrasonication, and then $MoO_2(acac)_2$ (0.004 g, 0.012 mmol) and TMEDA (0.001 g, 0.008 mmol) were added under stirring to form a clear yellow solution, to which $nBuPO_3H_2$ (0.004 g, 0.029 mmol) was added under stirring. The resulting mixture was left at room temperature for 48 h before filtration to give a yellow solution. Slow evaporation of this solution afforded the product as yellow crystals. Yield: ca. 23 % (based on $nBuPO_3H_2$). Elemental analysis (%) calcd for $C_{146}H_{351}N_3P_7S_{28}Mo_2Ag_{51}O_{48.5}$: C 18.06, H 3.64, N 0.29; found: C 18.27, H 3.51, N 0.38.

3: *t*BuSAg (0.035 g, 0.18 mmol) and $AgBF_4$ (0.004 g, 0.024 mmol) were dissolved in 6 mL methanol and dichloromethane under ultrasonication. Then $MoO_2(acac)_2$ (0.002 g, 0.006 mmol) and TMEDA (0.001 g, 0.008 mmol) were added under stirring to form a clear yellow solution, to which $nBuPO_3H_2$ (0.005 g, 0.036 mmol) was added. The resulting mixture was left at room temperature for 24 h without stirring, and a yellow solution was collected by filtration. Slow evaporation of this solution afforded the product as yellow crystals. Yield: ca. 40 % (based on $nBuPO_3H_2$). Elemental analysis (%) calcd for $C_{134}H_{318}P_8S_{30}MoAg_{48}O_{34}$: C 17.97, H 3.58; found: C 17.71, H 3.27.

Acknowledgements

We gratefully acknowledge financial support by National Natural Science Foundation of China (No. 21201067 and 51472095).

Keywords: cage compounds · clusters · phosphonates · silver · thiolates

How to cite: *Angew. Chem. Int. Ed.* **2015**, *54*, 15176–15180
Angew. Chem. **2015**, *127*, 15391–15395

- [1] a) L. C. Roof, J. W. Kolis, *Chem. Rev.* **1993**, *93*, 1037; b) A. Dolbecq, E. Dumas, C. R. Mayer, P. Mialane, *Chem. Rev.* **2010**, *110*, 6009.
- [2] a) D. Rais, J. Yau, D. M. P. Mingos, R. Vilar, A. J. P. White, D. J. Williams, *Angew. Chem. Int. Ed.* **2001**, *40*, 3464; *Angew. Chem.* **2001**, *113*, 3572; b) S.-D. Bian, H.-B. Wu, Q.-M. Wang, *Angew. Chem. Int. Ed.* **2009**, *48*, 5363; *Angew. Chem.* **2009**, *121*, 5467; c) F. Gruber, M. Jansen, *Angew. Chem. Int. Ed.* **2010**, *49*, 4924; *Angew. Chem.* **2010**, *122*, 5044; d) R. S. Dhayal, J.-H. Liao, Y.-C. Liu, M.-H. Chiang, S. Kahlal, J.-Y. Saillard, C. W. Liu, *Angew. Chem. Int. Ed.* **2015**, *54*, 3702; *Angew. Chem.* **2015**, *127*, 3773.
- [3] a) D. Fenske, C. Persau, S. Dehnen, C. Anson, *Angew. Chem. Int. Ed.* **2004**, *43*, 305; *Angew. Chem.* **2004**, *116*, 309; b) C. Anson, A. Eichhofer, I. Issac, D. Fenske, O. Fuhr, P. Sevilano, C. Persau, D. Stalke, J. Zhang, *Angew. Chem. Int. Ed.* **2008**, *47*, 1326; *Angew. Chem.* **2008**, *120*, 1346; c) K. Zhou, C. Qin, H.-B. Li, L.-K. Yan, X.-L. Wang, G.-G. Shan, Z.-M. Su, C. Xu, X.-L. Wang, *Chem. Commun.* **2012**, *48*, 5844; d) H. Yang, Y. Wang, H. Huang, L. Gell, L. Lehtovaara, S. Malola, H. Häkkinen, N. F. Zheng, *Nat. Commun.* **2013**, *4*, 2422; e) G. Li, Z. Lei, Q.-M. Wang, *J. Am. Chem. Soc.* **2010**, *132*, 17678; f) S. Jin, S. Wang, Y. Song, M. Zhou, J. Zhong, J. Zhang, A. Xia, Y. Pei, M. Chen, P. Li, M. Zhu, *J. Am. Chem. Soc.* **2014**, *136*, 15559.
- [4] a) M. G. Walawalkar, W. Roesky, R. Murugavel, *Acc. Chem. Res.* **1999**, *32*, 117; b) K. J. Gagnon, H. P. Perry, A. Clearfield, *Chem. Rev.* **2012**, *112*, 1034; c) F. A. Almeida Paz, J. Klinowski, S. M. F. Vilela, J. P. C. Tomé, J. A. S. Cavaleiro, J. Rocha, *Chem. Soc. Rev.* **2012**, *41*, 1088; d) A. Clearfield, *Prog. Inorg. Chem.* **1998**, *47*, 371; e) S. Konar, N. Bhuvanesh, A. Clearfield, *J. Am. Chem. Soc.* **2006**, *128*, 9604; f) V. Chandrasekhar, T. Senapati, A. Dey, E. C. Sañudo, *Inorg. Chem.* **2011**, *50*, 1420; g) P. O. Adelani, T. E. Albrecht-Schmitt, *Inorg. Chem.* **2011**, *50*, 12184.
- [5] a) *Metal Phosphonate Chemistry: From Synthesis to Applications*; (Eds.: A. Clearfield, K. Demadis), Cambridge, RSC Publishing, **2012**; b) Y.-Z. Zheng, M. Evangelisti, F. Tuna, R. E. P. Winpenny, *J. Am. Chem. Soc.* **2012**, *134*, 1057; c) L. Zhang, R. Clérac, P. Heijboer, W. Schmitt, *Angew. Chem. Int. Ed.* **2012**, *51*, 3007; *Angew. Chem.* **2012**, *124*, 3062; d) J. A. Sheikh, H. S. Jena, A. Adhikary, S. Khatua, S. Konar, *Inorg. Chem.* **2013**, *52*, 9717; e) E. Moreno Pineda, F. Tuna, R. G. Pritchard, A. C. Regan, R. E. P. Winpenny, E. J. L. McInnes, *Chem. Commun.* **2013**, *49*, 3522; f) J. Goura, V. Chandrasekhar, *Chem. Rev.* **2015**, *115*, 6854.
- [6] a) A. Clearfield, *New Developments in Ion Exchange Materials* (Eds.: M. Abe, T. Kataoka, T. Suzuki), Kodansha, Ltd., Tokyo, Japan, **1991**; b) G. Cao, H. Hong, T. E. Mallouk, *Acc. Chem. Res.* **1992**, *25*, 420; c) J.-G. Mao, *Coord. Chem. Rev.* **2007**, *251*, 1493.
- [7] a) Y.-P. Xie, T. C. W. Mak, *J. Am. Chem. Soc.* **2011**, *133*, 3760; b) Y.-P. Xie, T. C. W. Mak, *Angew. Chem. Int. Ed.* **2012**, *51*, 8783; *Angew. Chem.* **2012**, *124*, 8913; c) Y.-P. Xie, H. Wang, T. C. W. Mak, *J. Cluster Sci.* **2012**, *23*, 727; d) Y.-P. Xie, T. C. W. Mak, *Inorg. Chem.* **2012**, *51*, 8640.
- [8] Crystallographic data: **1**: orthorhombic, $a = 21.593(2)$, $b = 33.396(2)$, $c = 35.442(2)$ Å, $V = 25558(3)$ Å³, $T = 173$ K, space group $Pbcm$, $Z = 4$, $\lambda = 0.71073$ Å, $\rho = 2.286$ cm⁻³, $\mu(Mo_{K\alpha}) = 3.881$ mm⁻¹, $R_1 = 0.0963$, $wR_2 = 0.2099$ for $I > 2\sigma(I)$, GOF = 1.060. **2**: monoclinic, $a = 36.537(9)$, $b = 23.241(6)$, $c = 34.634(9)$ Å, $\beta = 90.330(7)$, $V = 29409(1)$ Å³, $T = 173$ K, space group $C2m$, $Z = 2$, $\lambda = 0.71073$ Å, $\rho = 2.195$ cm⁻³, $\mu(Mo_{K\alpha}) = 3.673$ mm⁻¹, $R_1 = 0.0635$, $wR_2 = 0.1601$ for $I > 2\sigma(I)$, GOF = 1.050. **3**: tetragonal, $a = 21.6138(4)$, $b = 21.6138(4)$, $c = 26.3495(1)$ Å, $V = 12309.3(6)$ Å³, $T = 173$ K, space group $I4m$, $Z = 2$, $\lambda = 0.71073$ Å, $\rho = 2.417$ cm⁻³, $\mu(Mo_{K\alpha}) = 4.120$ mm⁻¹, $R_1 = 0.0634$, $wR_2 = 0.1509$ for $I > 2\sigma(I)$, GOF = 1.062. CCDC 1417995 (**1**), 1417996 (**2**), and 1417997 (**3**) contain the supplementary crystallographic data for this paper. These data can be obtained

free of charge from The Cambridge Crystallographic Data Centre.

- [9] a) E. V. Chubarova, M. H. Dickman, B. Keita, L. Nadjo, F. Miserque, M. Mifsud, I. W. C. E. Arends, U. Kortz, *Angew. Chem. Int. Ed.* **2008**, *47*, 9542; *Angew. Chem.* **2008**, *120*, 9685; b) N. V. Izarova, M. H. Dickman, R. Ngo Biboum, B. Keita, L. Nadjo, V. Ramachandran, N. S. Dalal, U. Kortz, *Inorg. Chem.* **2009**, *48*, 7504; c) P. Yang, Y. Xiang, Z. Lin, B. S. Bassil, J. Cao, L. Fan, Y. Fan, M.-X. Li, P. Jiménez-Lozano, J. J. Carbó, J. M. Poblet, U. Kortz, *Angew. Chem. Int. Ed.* **2014**, *53*, 11974; *Angew. Chem.* **2014**, *126*, 12168.
- [10] a) J. A. Bonadies, M. L. Kirk, M. S. Lah, D. P. Kessissoglou, W. E. Hatfield, V. L. Pecoraro, *Inorg. Chem.* **1989**, *28*, 2037; b) D. Mootz, M. Steffen, *Angew. Chem. Int. Ed. Engl.* **1981**, *20*, 196; *Angew. Chem.* **1981**, *93*, 211; c) S. P. Lewis, L. D. Henderson, B. D. Chandler, M. Parvez, W. E. Piers, S. Collins, *J. Am. Chem. Soc.* **2005**, *127*, 46; d) H. Deng, Y. Qiu, C. Daiguebonne, N. Kerbellec, O. Guillou, M. Zeller, S. R. Batten, *Inorg. Chem.* **2008**, *47*, 5866.

Received: August 12, 2015

Revised: September 10, 2015

Published online: November 18, 2015